INTERNATIONAL JOURNAL FOR NUMERICAL AND ANALYTICAL METHODS IN GEOMECHANICS, VOL. 20, 725–751 (1996)

EARTHQUAKE ANALYSIS OF GRAVITY DAMS BASED ON DAMAGE MECHANICS CONCEPT

S. VALLIAPPAN, M. YAZDCHI AND N. KHALILI

School of Civil Engineering, University of New South Wales, Sydney 2052, Australia

SUMMARY

In this paper, the seismic response analysis of concrete gravity dams is presented using the concept of Continuum Damage Mechanics. The analysis is performed using the finite element technique and a proper material degradation/damage model. The damage criterion used here is a second order tensor model based on elastic-brittle characterization and on a power function of the principal tensile stress. The methodology employed is shown to be computationally efficient and consistent in its treatment of both damage growth and propagation. Other important features considered in the analysis are: (1) dam–foundation interaction (2) appropriate modelling of joined rock mass using continuum damage mechanics, and (3) proper modelling of unbounded domain of foundation rock. The infinite media representation of the foundation material has been achieved by using doubly asymptotic approximation. The results of the analysis indicate that the seismic response of a damaged concrete dam could be significantly different from that of an undamaged one. In particular, the analysis shows that during a seismic event, the microstructure of a damaged zone can significantly change due to growth and propagation of microcracks.

KEY WORDS: damage mechanics; earthquakes; gravity dam; damage evolution; absorbing boundary; anisotropic behaviour

1. INTRODUCTION

Earthquake-resistant design of dams is particularly important in view of a number of catastrophic consequences such as loss of life and property, if the dam fails. To date, there have not been any reported cases of complete failures of concrete dams even under the strongest levels of ground shaking because concrete gravity dams are, in general, designed to perform satisfactorily under all kinds of loading. However, the past experience shows that the concrete dams may be damaged or cracked seriously by earthquakes even though they may not fail completely.[1,2] Typical examples of dams which have suffered serious fracture problems in the past are Koyna dam, India (1967), Hsingfengkiang dam, China (1962) and recently Sefid-Rud dam, Iran (1990). Therefore, it is important to study the dynamic behaviour of concrete dams subjected to earthquake loading.

The assessment of seismic behaviour of large-scale structures such as concrete gravity dams requires the use of non-linear material models. But, non-linear models are computationally expensive and time consuming. Hence, on physical grounds, a constitutive law should be realistic and on numerical grounds should be fast and easy to implement. In the case of unreinforced massive concrete structures such as gravity dams, the main non-linearity is due to the formation of cracks.

CCC 0363–9061/96/100725–27

Received 29 March 1995
Revised 2 February 1996

In the past, many investigators have studied the effect of cracking on the seismic response of concrete dams using the concept of fracture mechanics.[3-6] The concept of fracture mechanics requires complete details of the initiation and propagation of cracks within the dam and the location, dimensions and physical properties of fracture in the rock foundation. Besides, the numerical modelling of such individual fracture requires special techniques such as quarter-point elements, remeshing, etc. Therefore, the application of fracture mechanics is limited to problems where only a few well-defined fracture are encountered. For large-scale problems such as concrete gravity dams where extensive microcracking may develop, it would be inefficient, especially in dynamic analysis.

In this paper, the concept of continuum damage mechanics is used to study the effect of microcracking on the seismic response of concrete gravity dams. Damage mechanics provides an average measure of material degradation due to microcracking, interfacial debonding, nucleation and coalescence of voids. In the microcracking of brittle materials under tensile stresses, damage is regarded as describing the elastic degradation. This material degradation is reflected in the non-linear behaviour of the structures.

The damage model used in this paper is a second-order tensor, elastic-brittle model. This model is preferred to the fourth-order tensor models due to the simplicity and the ease of use. The fourth-order model, in general, produces a large number of additional state variables which can be computationally expensive. It also introduces a far larger number of degrees of freedom than are needed to characterize accurately damage effects in many engineering applications.[7] The damage model employed here is capable of describing the rate-dependent non-linear behaviour or brittle materials. The damage accumulation is simulated by the continuous degradation of material stiffness during the loading process and is calculated using a power function of the principal tensile stresses.

The effect of damage has been considered both in the dam and the foundation materials. Other important features considered in the analysis are: (1) dam–foundation interaction and (2) infinite media representation of the foundation material. The dam–foundation interaction was modelled by extending the near-field zone of discretization into the foundation material. The infinite media representation of the unbounded domains is achieved using static infinite elements along with a series of absorbing boundary dashpots.

The results of the analysis indicate that the seismic response of a damaged concrete dam could be significantly different from that of undamaged dam. The seismic waves travelling through a gravity dam would result in the elevation of stresses in the damaged zones or in the local regions surrounding cracks and defects. In particular, the analysis showed that during a seismic event, the microstructure of a damaged zone can significantly change due to the growth and propagation of microcracks.

2. EQUATIONS OF MOTION FOR ANISOTROPIC DAMAGE MATERIALS

The equation of motion for the seismic analysis of an anisotropic damaged body can be written as[8]

$$[M]\{\ddot{U}\} + [C^*(D(t))]\{\dot{U}\} + [K^*(D(t))]\{U\} = \{P_{\text{eff}}(t)\} \tag{1}$$

where

$$[M] = \int_{v_e} \varrho [N]^{\mathrm{T}} [N] \, \mathrm{d}v \tag{2}$$

is the mass matrix for a damaged element. Also ϱ and $[N]$ represent mass density and shape function matrix, respectively. $[C^*(D(t))]$ is the time-dependent damping matrix, and

$$[K^*(D(t))] = \int_{v_e} [B]^T [T_\sigma][\tilde{E}^*][T_\sigma]^T [B]\, dv \tag{3}$$

is the time-dependent stiffness matrix for an anisotropic damaged element, $[T_\sigma]$ is the co-ordinate transformation matrix, $[\tilde{E}^*]$ is the damaged constitutive matrix in the orthotropic damage space, which will be derived in the following section and $\{P_{\text{eff}}(t)]$ is called the effective earthquake load.

The earthquake excitation of a system may be defined as a base rock excitation or as a rigid-base excitation. In the first case, the dynamic input can be applied in one of the following ways: (a) acceleration history, (b) velocity history, (c) stress (or pressure) history, or (d) force history applied at the rock base or a certain boundary surface. One restriction when applying velocity or acceleration input at a boundary is that such a boundary cannot be an absorbing boundary also. To circumvent this, a stress boundary condition can be used instead (e.g. a velocity record can be transformed into a stress record and applied to a quiet boundary), and in this case, a velocity history obtained at the boundary may be different than that from the original velocity record, because of the one-dimensional approximation of transformation. In the second case, earthquake acceleration is transformed to body force. The second approach is commonly used because in most cases only the free-field motions are known. Assuming that the free-field excitation at the interface of foundation and structure results from a rigid-body motion $u^G(t)$, the load vector due to earthquake excitation is given by

$$\{P_{\text{eff}}(t)\} = -\begin{bmatrix} m_{ss} & m_{sg} & 0 \\ m_{gs} & m_{gg} & 0 \\ 0 & 0 & 0 \end{bmatrix} \begin{Bmatrix} T_s^G \\ T_g^G \\ 0 \end{Bmatrix} \ddot{u}^G(t) \tag{4}$$

where m_{ij} are the mass matrices of the concrete dam only, the indices s and g mark the degrees of freedom of the structure and those shared by structure and foundation, respectively, while the index G stands for the rigid-body motion. The matrices T_i^G, $i = s, g$ contain the geometrical transformation between the structure and the free-field motion $u^G(t)$. Also $\ddot{u}^G(t)$ is the acceleration time history of an earthquake.

3. DAMAGE MODEL AND CONSTITUTIVE LAW FOR ANISOTROPIC DAMAGE STATE

Since the equivalent strain concept[9] is not applicable to an anisotropic damage state, Valliappan *et al.*,[10] using the principal anisotropic damage tensor and the unsymmetric effective stress tensor based on equivalent internal forces and equivalent complementary elastic energy, have developed a symmetric complete anisotropic elastic damage constitutive matrix. Using the fact that the internal forces acting on any damaged section are the same as the one before damage, the following relashionships hold:

$$\sigma_{ij}\delta_{jk}A_k = \sigma_{ij}^*\delta_{jk}A_k^* \tag{5}$$

where σ_{ij} and σ_{ij}^* are the components of Cauchy stress and net stress tensors and A_k and A_k^* indicate the undamaged and damaged areas with unit normal n_i and n_i^*, respectively. δ_{ij} is Kronecker delta function. Equation (5) can be rewritten as

$$\{\tilde{\sigma}^*\} = [\Psi]\{\tilde{\sigma}\} \tag{6}$$

where the stress vectors $\{\tilde{\sigma}^*\}$ and $\{\tilde{\sigma}\}$ are defined in the anisotropic co-ordinate system and

$$[\Psi] = \begin{bmatrix} \dfrac{1}{1-D_1} & 0 & 0 \\ 0 & \dfrac{1}{1-D_2} & 0 \\ 0 & 0 & \dfrac{1}{1-D_2} \\ 0 & 0 & \dfrac{1}{1-D_1} \end{bmatrix} \tag{7}$$

where D_1 and D_2 stand for damage parameters in principal anisotropic damage space. In fact, these two scalars represent damage value in the two principal stress directions. Equation (6) can be considered as the relation that transforms the Cauchy stress vector to the net stress vector in a 2-D anisotropic damage model.

Equation (6) is presented in the principal anisotropic coordinate system. In practical applications, it should be transformed into the geometric co-ordinate system of the structure. The co-ordinate transformation for the Cauchy stress vector can be given as

$$\{\sigma\} = [T_\sigma]\{\tilde{\sigma}\} \tag{8}$$

in which $\{\sigma\}$ is the Cauchy stress vector in global co-ordinate system.

The general transformation matrix of co-ordinates in 2-D space is

$$[T_\sigma] = \begin{bmatrix} \cos^2\theta & \sin^2\theta & -\sin 2\theta \\ \sin^2\theta & \cos^2\theta & \sin 2\theta \\ 0{\cdot}5\sin 2\theta & -0{\cdot}5\sin 2\theta & \cos 2\theta \end{bmatrix} \tag{9}$$

in which θ is the angle of anisotropy.

The co-ordinate transformation for the effective stress vector can be given as

$$\{\sigma^*\} = [T_\sigma^*]\{\tilde{\sigma}^*\} \tag{10}$$

The transformation matrix for the effective stress vector is a (4×4) in two dimensions. Substituting equations (8) and (10) into equation (6), the relashionship between the effective stress vector and the Cauchy stress vector in global co-ordinate system can be presented as

$$\{\sigma^*\} = [\Phi^*]\{\sigma\} \tag{11}$$

where

$$[\Phi^*] = [T_\sigma^*][\Psi][T_\sigma]^{-1} \tag{12}$$

and has the following form:

$$[\Phi^*] = \begin{bmatrix} \dfrac{\cos^2\theta}{(1-D_1)} + \dfrac{\sin^2\theta}{(1-D_2)} & 0 & \left(\dfrac{1}{1-D_1} - \dfrac{1}{1-D_2}\right)\dfrac{\sin 2\theta}{2} \\ 0 & \dfrac{\sin^2\theta}{(1-D_1)} + \dfrac{\cos^2\theta}{(1-D_2)} & \left(\dfrac{1}{1-D_1} - \dfrac{1}{1-D_2}\right)\dfrac{\sin 2\theta}{2} \\ \left(\dfrac{1}{1-D_1} - \dfrac{1}{1-D_2}\right)\dfrac{\sin 2\theta}{2} & 0 & \dfrac{\sin^2\theta}{(1-D_1)} + \dfrac{\cos^2\theta}{(1-D_2)} \\ 0 & \left(\dfrac{1}{1-D_1} - \dfrac{1}{1-D_2}\right)\dfrac{\sin 2\theta}{2} & \dfrac{\cos^2\theta}{(1-D_1)} + \dfrac{\sin^2\theta}{(1-D_2)} \end{bmatrix} \tag{13}$$

In order to obtain the constitutive relation pertinent to the anisotropic damage model in 2-D space, the complementary elastic energy of the damage state is reasonably assumed to be equal to the one of the undamaged state. Hence, the elastic constitutive relation in two-dimensional case can be represented as in[11]

$$\{\tilde{\sigma}\} = [\tilde{E}^*]\{\tilde{\varepsilon}\} \tag{14}$$

where

$$[\tilde{E}^*] = \begin{bmatrix} \dfrac{E_1(1-D_1)^2}{1-v_1v_2} & \dfrac{E_2(1-D_1)(1-D_2)v_1}{1-v_1v_2} & 0 \\ \dfrac{E_1(1-D_1)(1-D_2)v_2}{1-v_1v_2} & \dfrac{E_2(1-D_2)^2}{1-v_1v_2} & 0 \\ 0 & 0 & \dfrac{2G(1-D_1)^2(1-D_2)^2}{(1-D_1)^2+(1-D_2)^2} \end{bmatrix} \tag{15}$$

and using the transformation matrix the above constitutive relationship can be transformed from the anisotropic damage state into the global co-ordinate system. Then, the constitutive relation for an anisotropic damage model in a 2-D space can be written as

$$\{\sigma\} = [E^*]\{\varepsilon\} \tag{16}$$

where

$$[E^*] = [T_\sigma][\tilde{E}^*][T_\sigma]^T \tag{17}$$

Final constitutive equation of (15) includes damage due to tensile as well as shear deformations and $[\tilde{E}^*(3,3)]$ represents the shear resistance of the damaged material. It can be written in a manner similar to that of the smeared crack approach, $[\tilde{E}^*(3,3)] = \beta G$ where β is the shear retention factor and is a function of damage scalars D_1 and D_2. Also when we have compressive stress the material has its original strength ($D = 0{\cdot}0$), unless under high compressive stresses, crushing occurs, which is not usually the case in earthquake loading.

4. DAMAGE EVOLUTION

For the complete dynamic analysis of damaged materials, besides the appropriate constitutive law, it is necessary to specify the damage kinetic equation of the form

$$\dot{D} = \dot{D}(\sigma_{ij}, D, \dots) \tag{18}$$

where σ_{ij} is the state of stress at a particular point and D is the damage tensor at that point. Also $\dot{D}$ represents the rate of damage. The most common damage kinetic equation that is used widely is based on power function of tensile normal stress and was introduced first by Kachanov.[12] The above-mentioned function is employed here for unidirectional loading as

$$\dot{D} = \begin{cases} A\left(\dfrac{\sigma}{1-D}\right)^n, & \sigma > \sigma_d \\ 0, & \sigma \leqq \sigma_d \end{cases} \tag{19}$$

where $A > 0$, $n > 1$ are material constants depending on the rate of loading, σ is the uniaxial tensile stress, and σ_d is the stress at damage threshold. In the case of brittle materials, σ_d is static fracture strength of the material. The factor $(1 - D)$ is introduced to account for the acceleration of the damage accumulation rate with reduction in the effective area under load. For a given stress history, equation (19) can be integrated with respect to time to obtain D.

For the case of multiaxial state of stress and for isotropic damage, it is better to use the concept of equivalent stress of a Cauchy stress tensor based on von-Mises criterion, σ_{eq}. Then,

$$\dot{D} = \begin{cases} A\left(\dfrac{\sigma_{eq}}{1-D}\right)^n, & \sigma_{eq} > \sigma_{deq} \\ 0, & \sigma_{eq} \leqq \sigma_{deq} \end{cases} \tag{20}$$

where

$$\sigma_{eq} = \left\{\frac{1}{2}\left[(\sigma_x - \sigma_y)^2 + (\sigma_y - \sigma_z)^2 + (\sigma_z - \sigma_x)^2 + 6(\sigma_{xy}^2 + \sigma_{yz}^2 + \sigma_{zx}^2)^2\right]\right\}^{1/2} \tag{21}$$

and σ_{deq} is the threshold stress corresponding to Cauchy equivalent stress. Kachanov[12] has considered the extension of the above kinetic equation to the case of anisotropic materials. The kinetic equations corresponding to equation (19) in the anisotropic principal axes system are as follows:[12]

$$\dot{D} = \begin{cases} A_i\left(\dfrac{\sigma_i}{1-D_i}\right)^{n_i}, & \sigma_i > \sigma_{di}; \quad i = 1,2,3 \\ 0 & \sigma_i \leqq \sigma_{di} \end{cases} \tag{22}$$

where $A_i > 0$, $n_i > 1$ $(i = 1, 2, 3)$ are material constants in the direction of anisotropic principal axes, and σ_{di} represents threshold stress in ith principal direction. It is assumed that the principal axes of damage maintain a prescribed orientation in a material-fixed co-ordinate system and that the damage accumulation on the principal planes depends only upon the applied tensile stress. The rotation of principal axes after damage is negligible for all practical purposes. Therefore, the assumption of fixed orientation of principal axes is reasonable. It should be noted that the material constants A_i and n_i may be obtained from experimental results as will be explained in the next section.

In the finite element analysis, the stress distribution and the damage in an element are functions of time and co-ordinates. So it is difficult to carry out the necessary integrations of kinetic equations. In order to overcome this difficulty, an average damage value $\bar{D}$ and an average damage rate $\dot{\bar{D}}$ for isotropic case and $\bar{D}_i$ and $\dot{\bar{D}}_i$ for anisotropic case in a specified element can be used. Then the damage growth law in an element can be approximately developed for the general anisotropic case using the average value

$$\frac{\mathrm{d}\bar{D}_i}{\mathrm{d}t} = \begin{cases} \dfrac{A_i}{(1-\bar{D}_i)^{n_i}}\bar{\sigma}_i, & \sigma_i > \sigma_{\mathrm{d}i}; \quad i = 1,2,3 \\ 0 & \sigma_i \leqslant \sigma_{\mathrm{d}i} \end{cases} \tag{23}$$

where

$$\bar{\sigma}_i = \frac{1}{V_e}\int_{v_e} (\sigma_i)^{n_i}\,\mathrm{d}v \tag{24}$$

in which V_e is the volume of the element.

With the introduction of the above-mentioned approximation, the integration of equation (24) can be carried out using the Gauss-quadrature integration technique and accumulation of damage. In the two-dimensional case, the average of damage growth rate in an element at the jth time step can be represented using Heaviside function $H(x)$ as

$$\frac{\Delta\bar{D}_i^j}{\Delta t^j} = \frac{1}{A_e}\int_{A_e}\frac{A}{(1-\bar{D}_i^j)^n}[\sigma_i(x,y,t^j)]^{n_i} H[\sigma_i(x,y,t^j) - \sigma_{\mathrm{d}i}]\,\mathrm{d}A \tag{25}$$

in which A_e is the area of the element.

The contribution of $1/(1-\bar{D}^j)^n$ to the integration in equation (25) can be considered as a constant at time t^j. Thus, it can be taken out of the integration and the damage increment $\Delta\bar{D}^j$ for time increment t^j to t^{j+1} becomes

$$\Delta\bar{D}_i^j = \frac{A\Delta t^j}{A_e(1-\bar{D}_i^j)^n}\int_x\int_y [\sigma_i(x,y,t^j)]^{n_i} H[\sigma_i(x,y,t^j) - \sigma_{\mathrm{d}i}]\,\mathrm{d}x\,\mathrm{d}y \tag{26}$$

Using the Gaussian integration scheme, the integration in equation (26) can be defined as a function of

$$\Theta_n(t^j) = \frac{1}{A_e}\sum_{k=1}^{p}\sum_{l=1}^{p} W_k W_l [\sigma_i(\xi_k,\eta_l,t^j)]^{n_i} H[\sigma_i(\xi_k,\eta_l,t^j) - \sigma_{\mathrm{d}i}]\,|J| \tag{27}$$

where (ξ_k,η_l) and (W_k,W_l) are Gaussian points and weightings, respectively, $\sigma_i(\xi_k,\eta_l,t^j)$ is the normal stress at the Gaussian point (ξ_k,η_l) and at time t^j, and p is the number of Gauss points in each direction. Also $|J|$ is determinant of Jacobian matrix.

Therefore, the damage accumulation in an element at time $t = t^{j+1}$ can be calculated by the equation

$$\bar{D}_i^{j+1} = \bar{D}_i^j + \frac{A_i}{(1-\bar{D}_i^j)^{n_i}}\Theta_n(t^j)\cdot\Delta t^j; \quad i = 1,2,3 \tag{28}$$

It should be noted that in equation (28) superscript index j stands for time, while subscript index i stands for principal directions of damage tensor as mentioned earlier.

Once the material parameters and the time history of loading are specified in a structure, equation (28) can be employed to obtain the accumulated damage and hence proper estimation of structural behaviour under dynamic loading.

4.1. Calculation of parameters A and n

Parameters A and n may be evaluated from three-point bending tests with constant loading rate[13] applied to the reduced volume

$$V_r = \frac{V}{2(m+1)^2} \tag{29}$$

where V is the sample volume and m is a Weibull modulus[14]. As specimens increase in size the probability of fracture forming under otherwise equal stress conditions increases likewise. Based on the statistics of flaw distributions, Weibull[15] has derived a criterion which expresses j^{th} size sensitivity of specimen in the following way:

$$\frac{\sigma_1}{\sigma_2} = \left(\frac{V_2}{V_1}\right)^{1/m} \tag{30}$$

where σ_1 is the mean strength of volume V_1 and σ_2 is the mean strength of volume V_2. If m is large, the material is size sensitive. Weibull's theory has found its widest application in predicting failure behavior of brittle materials; for ductile materials the theory is hardly pertinent as long as static loads are applied. It can be shown, however, that a Weibull-type law may be obtained from the fracture criterion for dynamic loads.[16]

In uniaxial tension and for a constant loading (σ = constant), by solving the differential equation in equation (19) we obtain the time to failure as

$$\tau_{cs} = \frac{1-(1-D_c)^{n+1}}{(n+1)A\sigma^n} \tag{31}$$

where D_c is damage at fracture ($D_c \simeq 1$). For numerical stability reasons, the ultimate value of D_c is chosen as 0·99 here. The validity of following equation can be easily concluded from equation (31):

$$\frac{\tau_{cs1}}{\tau_{cs2}} = \left(\frac{\sigma_2}{\sigma_1}\right)^n \tag{32}$$

where σ_1 and σ_2 are two different applied stress levels on two identical samples which fail at times τ_{cs1} and τ_{cs2}, respectively. The above relation means the time to failure is inversely proportional to stress level to the power of n. Alternatively, the parameters A and n can be obtained from two constant strain rate ($\dot{\varepsilon}$ = constant) tests conducted on two samples. In this case we have the failure time of

$$\tau_{cr} = \left[\frac{1-(1-D_c)^{n+1}}{A(E\dot{\varepsilon})^n}\right]^{1/(n+1)} \tag{33}$$

or

$$\tau_{cr} = \frac{1-(1-D_c)^{n+1}}{A\sigma^n} \tag{34}$$

Equating equations (33) and (34) it can be shown that

$$\frac{\dot{\varepsilon}_1}{\dot{\varepsilon}_2} = \left(\frac{\sigma_1}{\sigma_2}\right)^{n+1} \tag{35}$$

Further it can be stated that for two different strain rates, the ratio of the two values of parameter A should be

$$\frac{A_1}{A_2} = \left(\frac{\sigma_2}{\sigma_1}\right)^{n+1} \tag{36}$$

Also comparison of equations (31) and (34) shows that

$$\frac{\tau_{cs}}{\tau_{cs}} = n + 1 \tag{37}$$

The above equation is valid for two identical samples, one loading with constant stress σ which fails at τ_{cs}, and another with constant strain rate at the same value of σ and failure time of τ_{cr}. Hence, to evaluate the parameters A and n, at least two dynamic tests with constant strain rates or constant stress are required. Doing these tests we obtain two sets of strain rate, failure stress and time to failure. Then using the above relations, these parameters are obtained. Further details of this test procedures are given by Fahrenthold.[7]

During an earthquake, dams are subjected to alternating excitations at high strain rates (10^{-4} to $1{\cdot}0\ s^{-1}$). From the experimental data and assuming the same material properties as in Yon[13], and considering the strain rate range that happens during earthquakes, material parameters A, n may be estimated, and hence damage evolution of (28) can be used to obtain accumulated damage under different loadings.

For the referenced experiments on concrete, it was found that the measured bending strengths at various strain rates were described by two-parameter Weibull distributions incorporating identical Weibull moduli (m) and differing in their mean strengths (σ_m). A Weibull model of failure, is based on the assumption that flaws are distributed at random with certain density per unit volume. So this model is ideal for application in damage mechanics. The failure is based on the 'weakest link hypothesis', which states that a component will fail when the stress intensity at any flaw reaches a critical value for crack propagation. Thus, the structural component is represented as a series model or a chain, with components being small parts of the structure, in which the failure depends on the weakest component.

For the expression of probability of failure a Weibull distribution[15] is used, and the probability of failure of a stressed volume V_s under a normal tensile stress σ is computed as[14]

$$P_f = 1 - \exp\left[-V_s\left(\frac{\sigma - \sigma_u}{\sigma_0}\right)^m\right] \tag{38}$$

where σ_0 and m (Weibull modulus) are material constants. They can be estimated from experimental data as shown by Dukes.[17] Also σ_u is threshold stress which materials can withstand without failure and hence is called zero probability stress. Intuitively, $\sigma_u = 0$ and this has been often found to be true experimentally.

In uniaxial tension, the stressed volume is expressed as[14]

$$V_s = \frac{V_r}{m + 1/2} \tag{39}$$

As mentioned earlier, the Weibull parameters σ_0 and m can efficiently show the effect of microcrack distribution within the material on the damage accumulation rate. In the finite element implementations of the above-mentioned damage evolution laws, equations (29) and (38) can be employed to modify experimentally measured material properties in order to take into account sample volume effects.

From the experimental work of Yon[13] on concrete in three-point bending test under ambient laboratory conditions with constant strain rates range 0·00045–0·252 s^{-1} which are in the same range as for earthquake excitations, the following material properties are obtained: $n = 12$; $A = 5{\cdot}394E - 9\ Pa^{-12}s^{-1}$.

5. INFINITE REGION

In order to model properly infinite region using the finite element technique, artificial boundary between the discretized near field of the foundation and the surrounding region have to be imposed such that the waves resulting from the excited source are not reflected from the boundaries back to the near field and should propagate to infinity. The best way to model infinite region is to use time-dependent infinite elements and coupled with finite elements. In this approach all characteristics of unbounded domain are included in the calculation, but to the best of the authors' knowledge this kind of infinite elements have not been developed so far. In the case of dynamic elasticity problems, normally two kinds of waves, dilatation and shear waves are involved. When a free surface is also present, the Rayleigh wave is also present, and if the medium is layered, Love waves may be present, all of which have different wave speeds. All these waves participate in all displacements, which makes numerical modelling highly complicated. It is possible to rewrite the equations in terms of potentials or stress functions[18] and in both cases, the different wave equations can be separated. However, in time domain, it is more difficult to formulate infinite elements in terms of such variables.

Another way of developing an infinite element is through Fourier transformation (frequency domain analysis), provided the problem is linear, by carrying out a series of periodic solutions and using numerical methods to inverse into a time domain which is not applicable for non-linear problems.

Some researchers have adopted the DDA (Doubly Asymptotic Approximation) in time domain to treat the problem.[19] A modification of DDA is explained herein. Two states are distinguished, the static state without any wave propagation and the dynamic state with energy radiation towards infinity. For each state, an approximation of the infinite domain exists. Combining these together, the so-called double asymptotic formulation is obtained. Thus, an approximation for the stiffness of the unbounded domain is obtained and the energy radiation is simulated by viscous damping forces at the artificial boundary.

5.1. The static state

Based on mapped infinite elements,[20] the infinite domain can be mapped into a parameter space by special geometric shape functions. In the parameter space, the unknown displacements are approximated by standard Lagrangian interpolation functions.

In two dimensions, for eight-node serendipity infinite element, according to Figure 1 the mapping function for node 8 ($\xi = -1{\cdot}0, \eta = 0{\cdot}0$) is the linear mapping function in ξ multiplied by the quadratic shape functions in η, that is

$$M_8 = (1 - \eta^2)\frac{2}{1 - \xi} \tag{40}$$

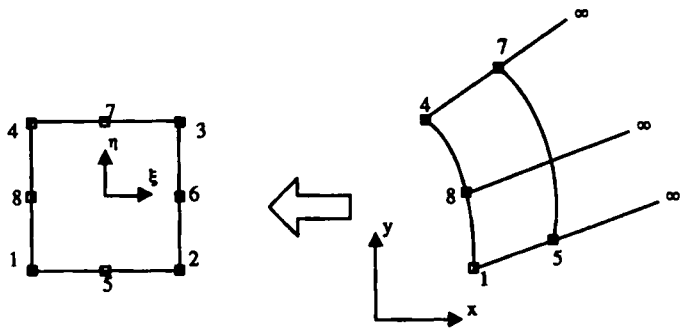

Figure 1. Two-dimensional geometric mapping used in mapped infinite elements

Similarly,

$$M_5 = (1-\eta)\frac{(1+\xi)}{2(1-\xi)}$$
$$M_7 = (1+\eta)\frac{(1+\xi)}{2(1-\xi)} \tag{41}$$

The infinite mapping functions for the nodes at the vertices ($\xi = -1, \eta = \pm 1$) are the product of linear mapping functions in the ξ direction and the linear shape functions in the η direction minus multiples of the midside node mapping functions. So

$$M_1 = (-1-\eta+\xi\eta+\eta^2)/(1-\xi)$$
$$M_4 = (-1-\xi+\xi\eta+\eta^2)/(1-\xi) \tag{42}$$

and nodes 2, 6 and 3 aproach to infinity. From these mapping functions, the Jacobian can be calculated for use in a finite element assemblage.

Geometry of the infinite element is transformed from local to the global co-ordinate system using

$$x = \sum_i M_i x_i, \quad i = 1,4,5,7,8$$
$$y = \sum_i M_i y_i, \quad i = 1,4,5,7,8 \tag{43}$$

Similarly, transformation for unknown functions are

$$u = \sum_{i=1}^{8} N_i u_i$$
$$v = \sum_{i=1}^{8} N_i v_i \tag{44}$$

where N_i is standard isoparametric shape function. The new co-ordinate interpolation function only affects the computational procedure for evaluating the Jacobian

$$J = \begin{bmatrix} \dfrac{\partial x}{\partial \xi} & \dfrac{\partial y}{\partial \xi} \\ \dfrac{\partial x}{\partial \eta} & \dfrac{\partial y}{\partial \eta} \end{bmatrix} \tag{45}$$

In this approach the usual Gauss quadrature integration scheme can be used for both finite elements as well as infinite elements. The remaining procedure for constructing element matrix is same as the finite element method.

5.2. *The dynamic state*

For the absorbing layer of the infinite element, White *et al.*[21] approach is used. No wave propagation can arise toward the interior region from infinity. In this method, the media encountered are assumed to be transversely anisotropic.

The boundary conditions for damping can be well expressed in the form proposed by Lysmer and Kuhlemeyer[22] as

$$\begin{aligned} \sigma_n &= a\varrho v_p \dot{u}_n \\ \tau &= b\varrho v_s \dot{u}_t \end{aligned} \tag{46}$$

where σ_n and τ are the normal and tangential stresses imposed by the boundary, $\dot{u}_n$ and $\dot{u}_t$ are the normal and tangential velocities at the boundary, a and b are the dashpot constants, and v_p and v_s are the velocities of 'P' and 'S' waves.

The systematic way of evaluating the values for the constants a and b in equation (46) for an isotropic medium has been described elsewhere[21] and not repeated here. Hence, only the details required for the anisotropic case are presented herein.[23]

Equation (42) may be rewritten alternatively in matrix form as

$$\begin{Bmatrix} \sigma_n \\ \tau \end{Bmatrix} = \begin{bmatrix} a\varrho v_p & 0 \\ 0 & b\varrho v_s \end{bmatrix} \begin{Bmatrix} \dot{u}_n \\ \dot{u}_t \end{Bmatrix} \tag{47}$$

or

$$\{\sigma_b\} = [C_b]\{\dot{u}_b\} \tag{48}$$

In general, matrix $[C_b]$ in equation (48) is presented as[21]

$$[C_b] = [E_b][B_b] \tag{49}$$

in which $[E_b]$ is appropriate stress–strain relation matrix and $[B_b]$ is strain–velocity matrix for the boundary.

For transversely anisotropic material, the stress and strain relation matrix can be written as[24]

$$[E_b] = \frac{E_2}{(1+\nu_1)(1-\nu_1-2m_1\nu_2^2)} \begin{bmatrix} m_1(1-m_1\nu_2^2) & m_1\nu_2(1+\nu_1) & 0 \\ 0 & 0 & m_2(1+\nu_1)(1-\nu_1-2m_1\nu_2^2) \end{bmatrix} \tag{50}$$

where $m_1 = E_1/E_2 = \nu_1/\nu_2$ and $m_2 = G/E_2$, E_1 and ν_1 are associated with behaviour in plane of strata, E_2 and ν_2 are associated with a direction normal to the strata, and G is the shear modulus of the material.

Matrix $[B_b]$ is expressed as

$$[B_b] = \frac{8}{15\pi}\begin{bmatrix} \frac{4}{V_p} + \frac{1}{V_s} & 0 \\ \frac{1}{V_p} - \frac{1}{V_s} & 0 \\ 0 & \frac{2}{V_p} + \frac{3}{V_s} \end{bmatrix} \tag{51}$$

where V_p and V_s in anisotropic case are given by

$$V_p = \sqrt{\frac{E_b(1,1)}{\varrho}} = \sqrt{\frac{E_2 m_1(1 - m_1\nu_2^2)}{(1+\nu_1)(1-\nu_1-2m_1\nu_2^2)\varrho}}$$

$$V_s = \sqrt{\frac{E_b(2,3)}{\varrho}} = \sqrt{\frac{E_2 m_2(1+\nu_1)(1-\nu_1-2m_1\nu_2^2)}{(1+\nu_1)(1-\nu_1-2m_1\nu_2^2)\varrho}} \tag{52}$$

The stresses at the boundary can be evaluated from equation (48) for any given values of E_1, E_2, G and ν_1. The product of $[E_b][B_b]$ in equation (49) is not generally diagonal. However, for the present plane strain case, the off-diagonal terms are zero because of antisymmetry in the relevant terms of matrix $[B_b]$.

Now, the parameters a and b in equation (47) are functions only of m_1 and ν_1 or ν_2. These parameters can be easily evaluated for a wide range of values of modular ratio and Poisson's ratio.

For isotropic state the above relation is simplified as

$$V_s = \sqrt{\frac{G}{\varrho}} \tag{53}$$

$$V_p = \frac{1}{S} V_s$$

where

$$S^2 = \frac{1-2\nu}{2(1-\nu)} \tag{54}$$

and ν is Poisson's ratio. Then the parameters a and b in isotropic case are expressed as

$$a = \frac{8}{15\pi}(5 + 2S - 2S^2) \tag{55}$$

$$b = \frac{8}{15\pi}(3 + 2S)$$

The above parameters were obtained by White *et al.*[21] and they are equal to 1 in standard boundary damping.[22]

The equivalent nodal forces due to the boundary stresses are

$$[F^{gm}] = -\int [N]^T \{\sigma_b\} \, d(\text{area}) \tag{56}$$

and the consistent geometric damping matrix for an element can be obtianed as

$$[C_{gm}] = \int [N]^T \{C_b\} [N] \, d(\text{area}) \tag{57}$$

in which the integration in carried out over the boundary area only. This matrix together with material damping consists damping matrix for elements located at boundary.

6. JOINED ROCK MASS MODELLING

Discontinuities such as cleavage cracks and defects are commonly encountered in rock mass and they have significant influence on the deformation and failure characteristics of rock. If a rock mass is embedded with a number of cracks which are not sufficiently small compared to the structure, the behaviour of the rock mass involving such cracks can be conveniently treated by describing the geometry of each crack and the properties of intact rock separately by characterizing the orientation and spacing of the cracks. The initial damage state may be estimated by appropriate laboratory tests or field measurements, as well as by approximate statistical methods, as has been developed by Kawamoto *et al.*[25] for rock mass.

According to Figure 2 if there are a small number of cracks with definite length and spacing (Figures 2(a) and 2(b)), then the continuum methods are unable to find out the behaviour of this kind of rock mass. In this case, the problem can be solved using joint elements[26,27] or distinct elements.[28] In the second case if there are small-sized crack compared to the structure being analysed (Figures 2(c) and 2(d)), the whole body can be idealized as a continua, and in this case either damage mechanics or any other numerical tools that are available might be used. The important role of damage mechanics appears when there are intermediate-sized cracks in the rock mass (Figure 2(e) and 2(f)).

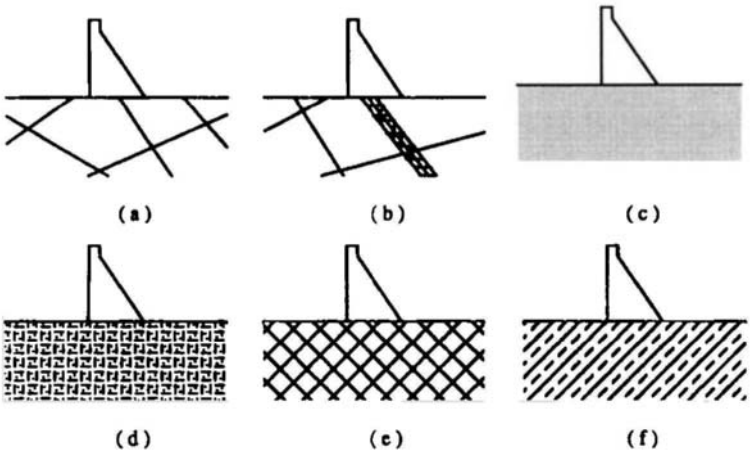

Figure 2. Discontinuities of dam foundation

If the discontinuities are distributed in a random fashion, an isotropic damage state may be reasonably adopted. However, if they are distributed in several definite directions the isotropic damage assumption is no longer valid and, hence, an anisotropic damage modelling is necessary. It is generally considered that the damage variable in isotropic damage model is a scalar, but for the complex defects and their distribution, it is necessary to use tensorial description of damage. In spite of above classifications, the major treatment of the cracks appear to be from a deterministic view point. The major parameters that affect the strength, and consequently the crack growth behaviour in engineering materials are of statistical nature.[29] Since the mechanical properties show some scatter, the resulting effect could be random in nature. However, in practice, the rock mass exhibits random damaged state (such as the random nature of length and number of cracks) and anisotropy (such as approximately parallel distribution or layered distribution of groups of cracks within a rock mass). The direction of cracks sometimes exhibits regular but random nature and the variation of the distribution of angle is not too significant. This results in the crack angle distribution becoming both random and anisotropic. Therefore, the distribution of the cracks in rock mass can be investigated based on a random and anisotropic damage state.

As mentioned above the initial state of damage may be estimated by statistical method, such as given by Kawamoto *et al.*[25] They determined the damage tensor by measurement of density, direction, and area of cross-section of the crack in a rock specimen sampled from a parent population of rock mass. Hence, damage tensor $[D]$ can be estimated in terms of observation of the average values of crack length L_i, L_j, number N_i, N_j and orientation n_i, n_j on three independent surfaces of a cube cracked rock specimen.[25]

7. NUMERICAL IMPLEMENTATION

The constitutive law and damage models described in the previous sections have been implemented into the dynamic Lagrangian finite element program.

In this method, the damage evolution in each element can be determined, thus making it possible to model both damage propagation and damage growth. The stress–strain law adopted for the brittle materials is as follows: at any time increment, if the principal stress within the element is compressive, then the original properties are considered to be valid for the constitutive relationship. On the other hand, if the tensile stress occurs, then, the material properties have to be changed in the direction (or directions) normal to the tensile stress. In other words, the stiffness matrix of the individual elements will be changed as the status of the cracks alternates from opening to closing. So at each time step an iterative procedure should be adopted to find out the state of stress in each element. Hence, the stiffness matrix of the system is changed at every time step. This step is very important, especially in the earthquake loading since the sign of stresses might be changed at every time step. During loading, the elements of damage tensor are accumulated for every time increment. The element stiffness at the end of the previous time step is used to compute the system stiffness matrix for the current time, with the consideration of brittle behaviour of materials as discussed earlier. The state of stress in each element is obtained and used in damage evolution laws to update the damage tensor components and the element stiffness matrix at every time step. An iterative algorithm is used to integrate the evolution equations and update the stresses at each time step. Consistent with the damage-based continuum approach used here, the element failure is defined by a minimum normal criterion

$$D_i = D_c; \quad i = 1, 2 \tag{58}$$

where D_i ($i = 1, 2$) are eigenvalues of damage tensor and D_c is the critical damage value. Hence, the damage tensor components calculated at each time step are compared to its critical value, D_c.

When equation (58) is satisfied for a specific element, it is assumed that failure occurs along a plane normal to the ith eigenvector of the damage tensor and has zero stiffness in that direction. When both D_1 and D_2 reach the value of D_c, the element is considered to have failed due to tension and it is assumed that the element is capable of supporting only the hydrostatic compressive stresses.

8. NUMERICAL RESULTS

A 80 m high concrete dam of vertical upstream face and downstream slop of $\simeq 1/0{\cdot}55$ subjected to horizontal base excitation is investigated. The dam is discretized with finite elements while the surrounding foundation with finite and infinite elements [Figure 3(a)]. The material properties of

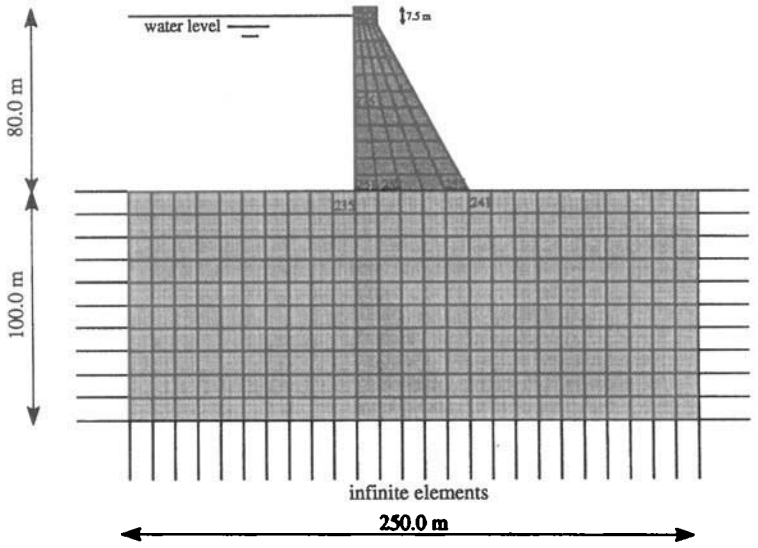

Figure 3(a). Geometry and discretization of dam–foundation system

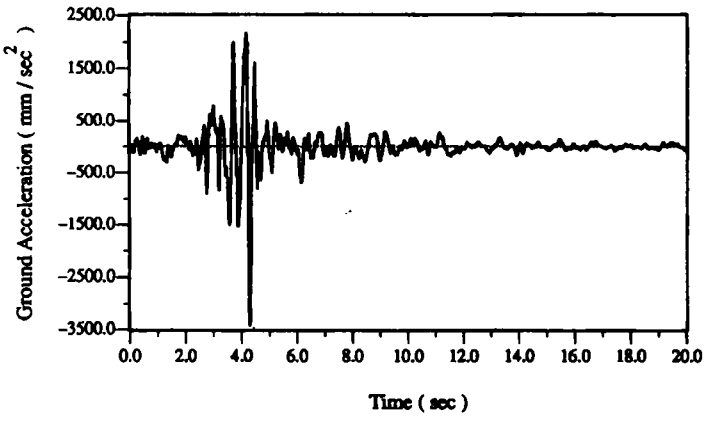

Figure 3(b). 1966 California Earthquake Accelogram

the system are as follows:

dam:	foundation:
$E = 2{\cdot}18 \times 10^{10}\ \mathrm{N/m^2}$	$E = 1{\cdot}52 \times 10^{10}\ \mathrm{N/m^2}$
$\nu = 0{\cdot}20$	$\nu = 0{\cdot}33$
$\varrho = 2500.0\ \mathrm{kg/m^3}$	$\varrho = 2400{\cdot}0\ \mathrm{kg/m^3}$

The viscous damping has been used in the finite element model with damping ratio of $\zeta = 0{\cdot}05$ for both dam and foundation. The 1966 California earthquake with horizontal acceleration as shown in Figure (3b) is used as a ground motion. In the first stage the system without preexisting microcracks is studied, and comparison has been made between the case where damage evolution is considered and the case without consideration of damage evolution (Figures 4–8). As indicated by Figure 4 due to stress concentration at the upstream corner damage mainly accumulated at this area, while in other areas damage is negligible when compared to highly stress concentrated zone. This is confirmed also by Figure 4(d) when time history of average damage rate is plotted.

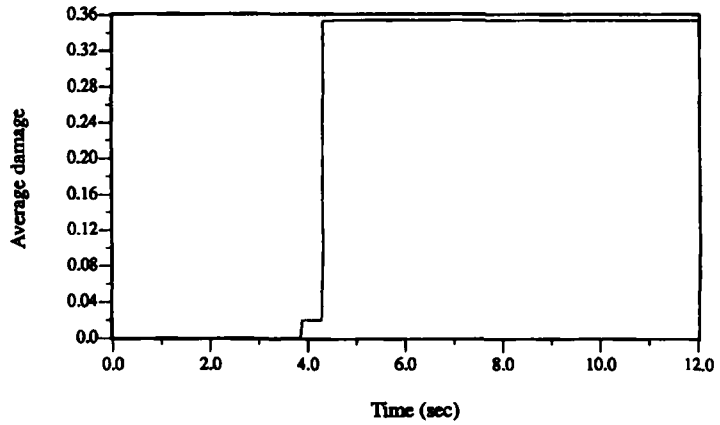

Figure 4(a). Average damage is element 251 during damage evolution without initial damage

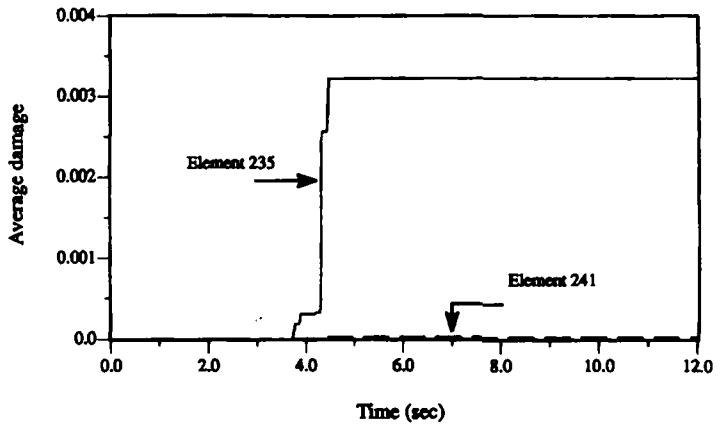

Figure 4(b). Average damage in some elements of foundation rock during damage evolution without initial damage

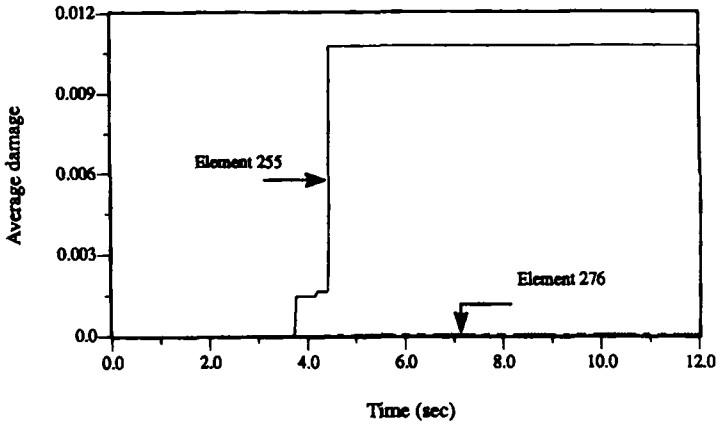

Figure 4(c). Average damage in some elements of concrete dam during damage evolution without initial damage

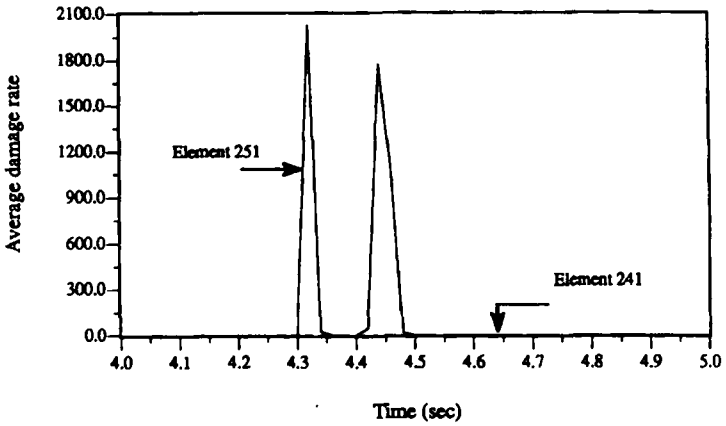

Figure 4(d). Average damage rate during damage growth

Figure 4(d) shows a jump in the time history of average damage rate at time $t = 4{\cdot}32$ s which is due to peak ground acceleration of $3{\cdot}408$ m/s^2. When a dam is subjected to earthquake loading, the transient stress waves are generated and propagated. The response due to dynamic loading can cause elevation of stress level specially in a damaged zone or in the local regions surrounding the cracks and the defects. This fact has been demonstrated by Figure 5(a). As is shown stress levels can increase as high as $1{\cdot}5$ times when damage evolution is considered. Figure 5(b) shows that there is not very much difference between net and Cauchy minor principal stress and this indicates that damage occurs mainly normal to the direction of the major principal stresses. In other words, microcracks are oriented in horizontal direction. Damage strain energy release rate and net von-Mises equivalent stress time histories in damaged zones have been plotted in Figure 6 and 7, respectively. It is evident that with increasing damage, more energy is stored in an element and hence is more susceptible to damage growth. According to Figure 8 during variation in microstructure of the system, displacements increase.

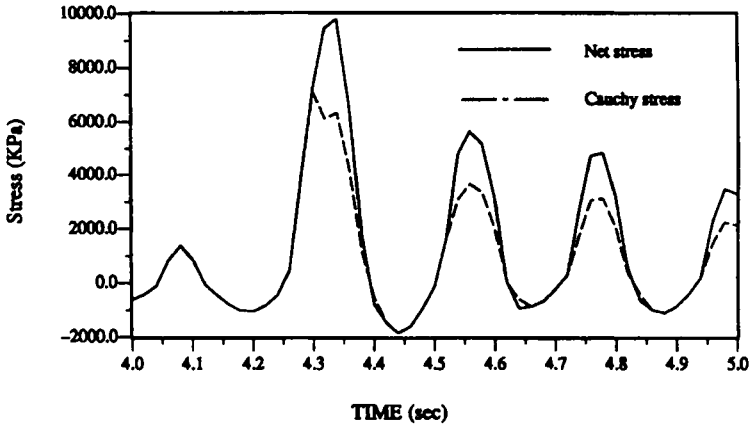

Figure 5(a). Net and Cauchy major principal stress in element 251 during damage evolution without initial damage

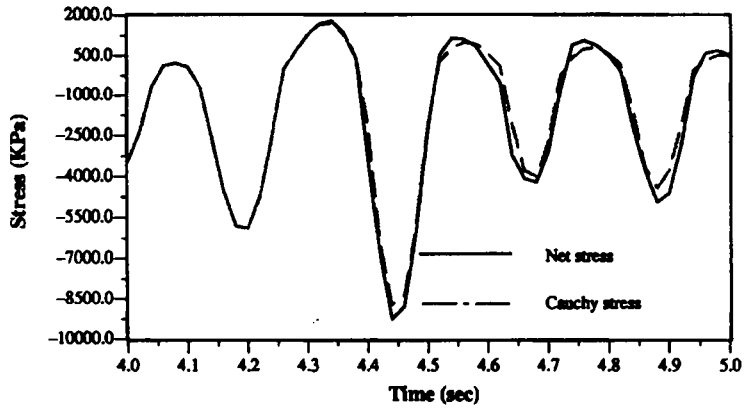

Figure 5(b). Minor principal stress in damaged zone during damage evolution without initial damage

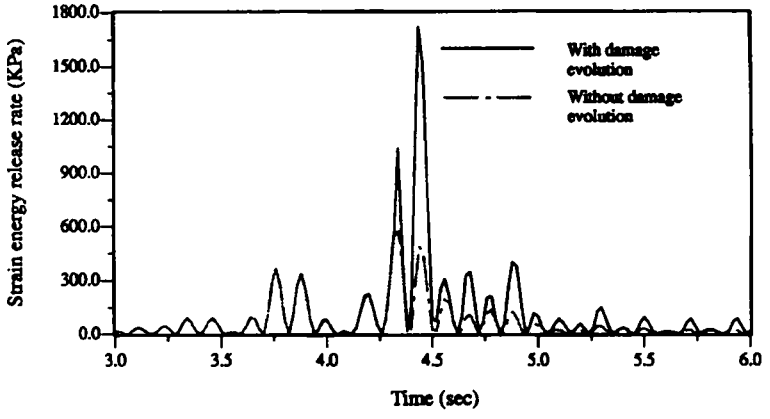

Figure 6. Damage strain energy release rate in damaged zone during damage evolution without initial damage

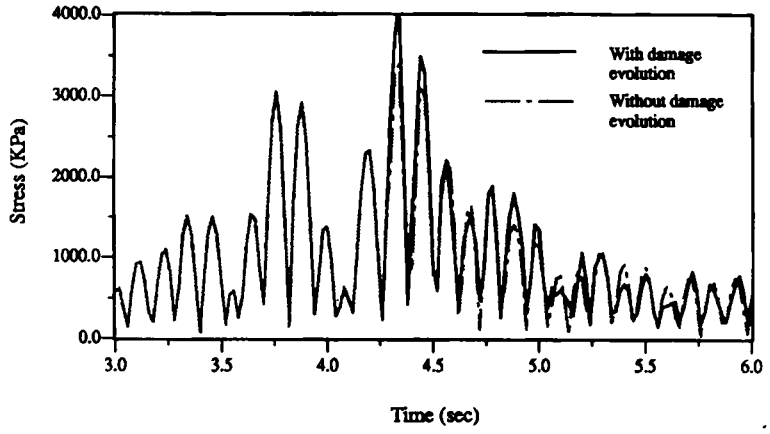

Figure 7. Net von-Mises equivalent stress at damaged zone during damage evolution without initial damage

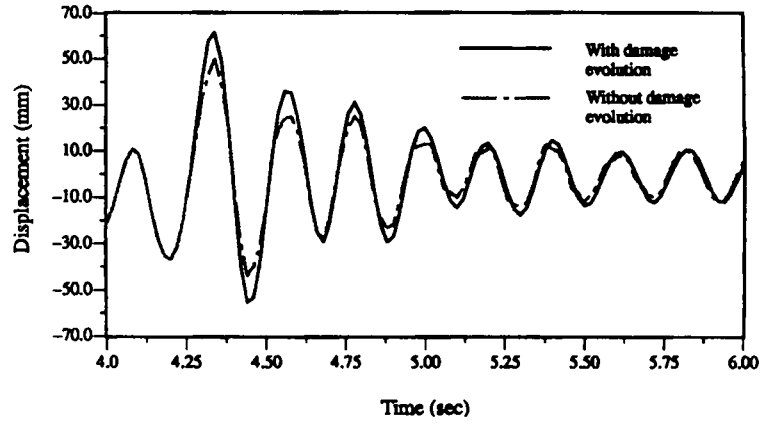

Figure 8. Horizontal displacement time history of crest during damage evolution without initial damage

In the second part of study, the effects of some initial microcracks (Figure (9)) is considered. The reasons for microcracking may be many fold, from them seismic actions of prior earthquakes is very important. The results of the analysis are given in Figures (10)–(13). As can be seen from these figures preexisting microcracks would result in a higher average damage. There would also be a higher level of stress and energy in damaged zone.

Finally, jointed rock mass modelling is investigated. The results of numerical simulation assuming an average initial damage of 0·1 in foundation rock are given in Figures 14–16. Maximum value of average damage in this case is lower than the first one, and this is due to the foundation effect. It can be said that we have softer material in this case comparing to intact rock mass, and hence can absorb the energy of generated waves due to earthquake. This is also confirmed by Figure 16. Contours in Figure 17 are the average damage values for the different cases, and show the growth of damaged zone at the end of the analysis. Also contours of Figure 18 show the distribution of net major principal stress at time $t = 4{\cdot}46$ s. As shown by these figures, there is a high stress concentration area in the upstream side as stated before, where the damage mainly grows.

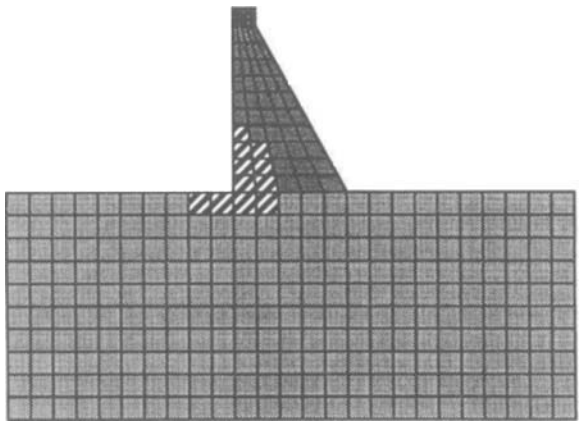

Figure 9. Initial damage in some areas with average value of 0·075

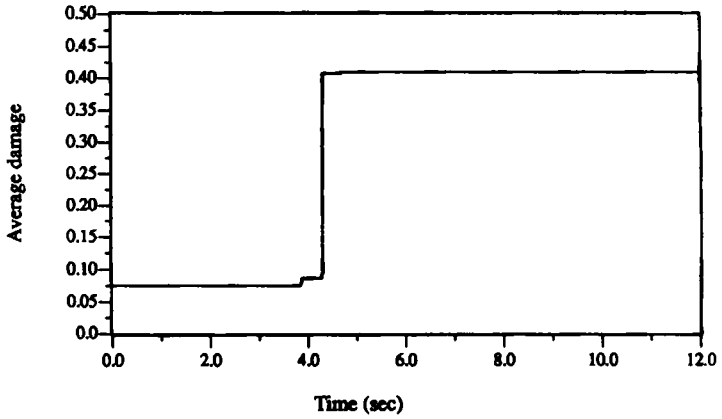

Figure 10. Average damage in element 251 during damage evolution with initial damage in some areas according to Figure 9

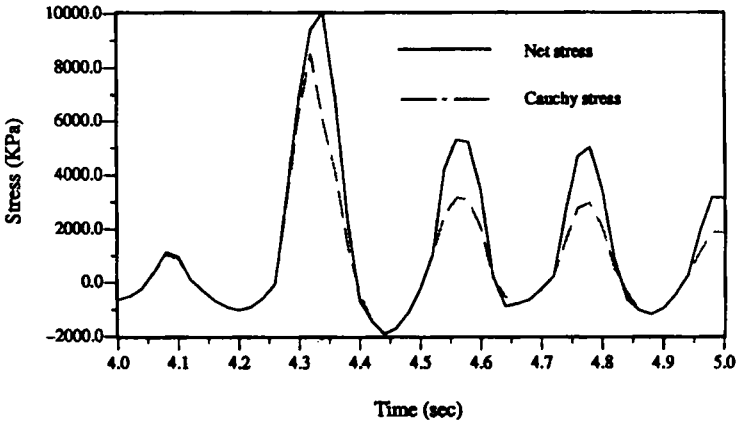

Figure 11. Net and Cauchy major principal stress in element 251 during damage evolution with initial damage in some areas according to Figure 9

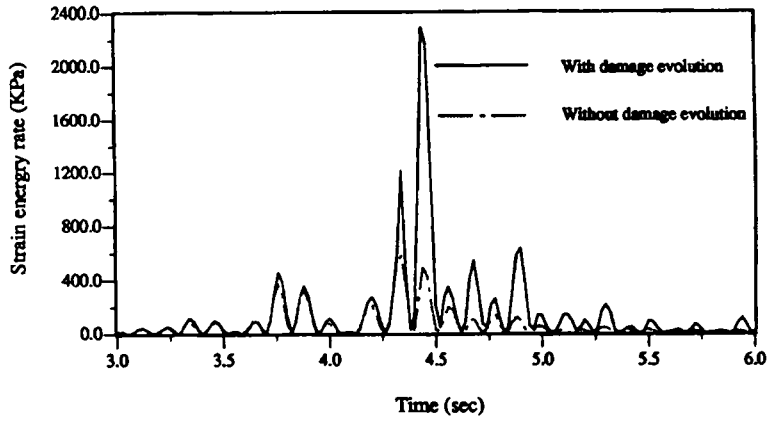

Figure 12. Damage strain energy release rate in damaged zone during damage evolution with initial damage in some areas according to Figure 9

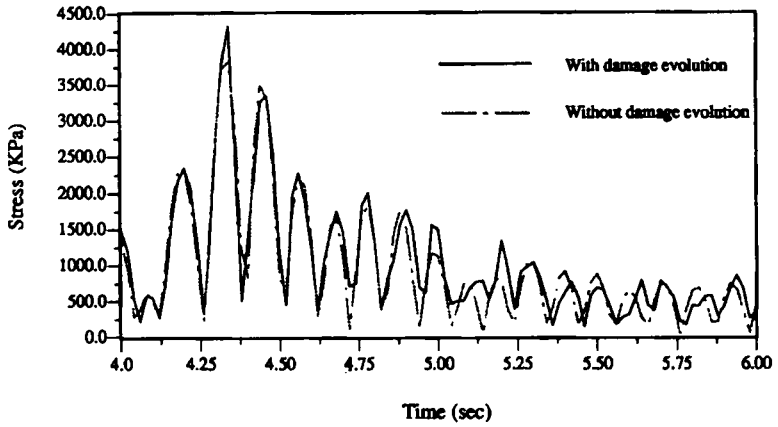

Figure 13. Net von-Mises equivalent stress during damage evolution with initial damage in some areas according to Figure 9

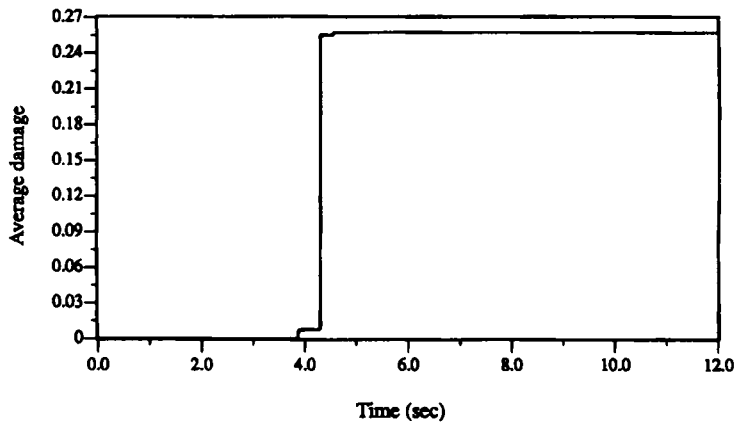

Figure 14. Average damage in element 251 during damage evolution with initial damage of 0·1 in foundation rock

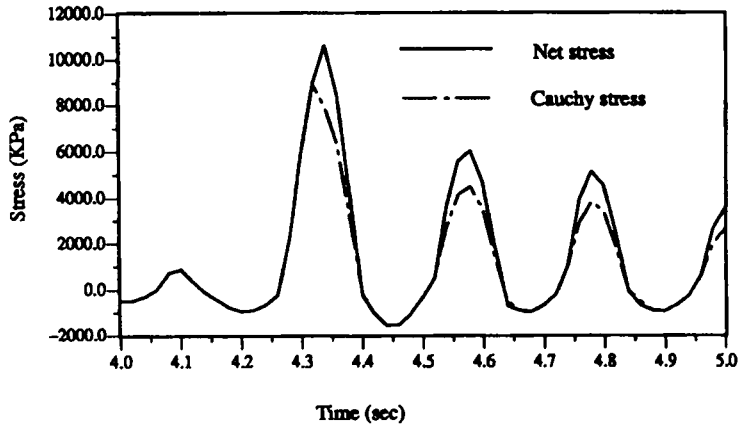

Figure 15. Net and Cauchy stresses in damaged area during damage evolution with initial damage of 0·1 in foundation rock elements

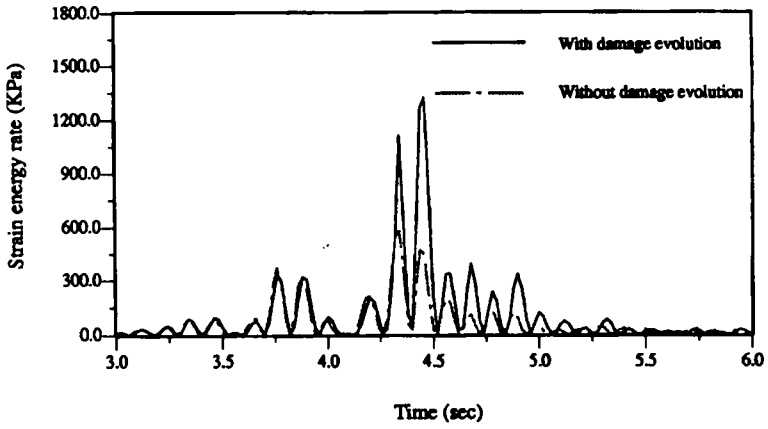

Figure 16. Damage strain energy release rate in damaged area during damage evolution with initial damage of 0·1 in foundation rock elements

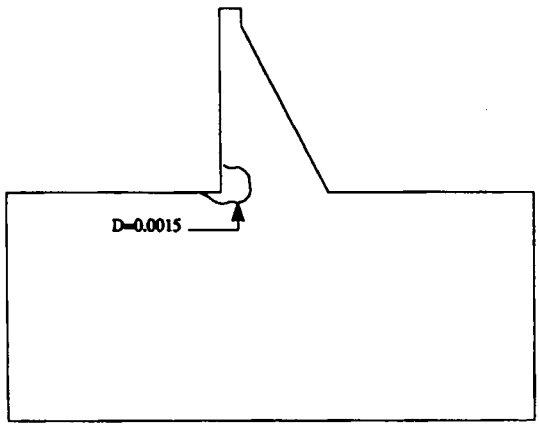

Figure 17(a). Average damage contour at time t = 12·0 s during damage evolution without initial damage and empty reservoir

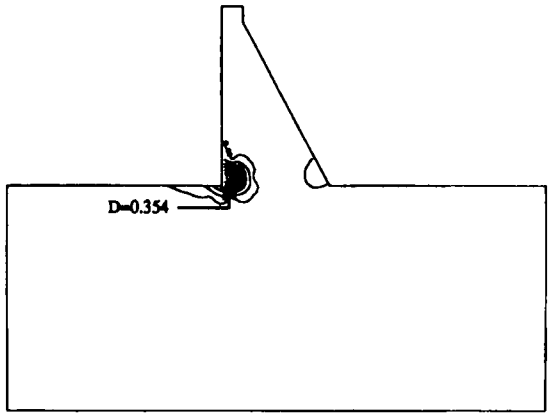

Figure 17(b). Average damage contour at time $t = 12{\cdot}0$ s during damage evolution without initial damage and full reservoir

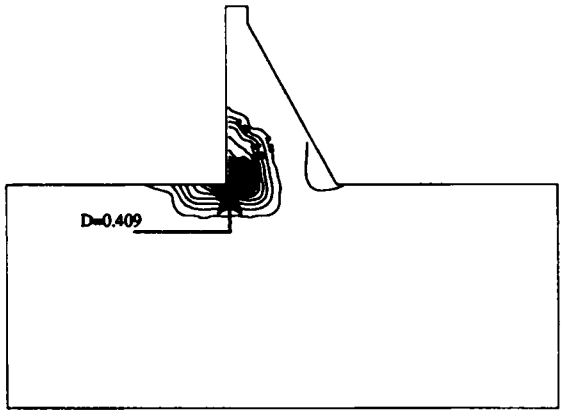

Figure 17(c). Average damage contour at time $t = 12{\cdot}0$ s with initial damage in some areas according to Figure 9

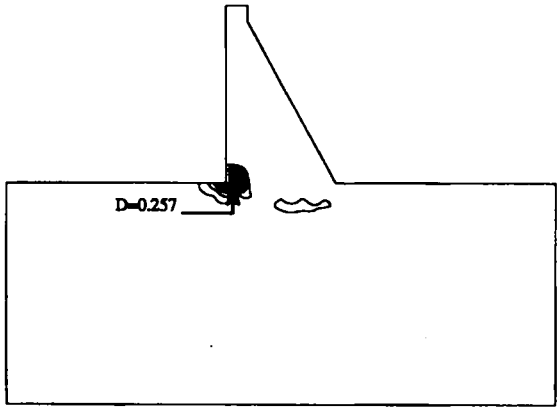

Figure 17(d). Average damage contour at time $t = 12{\cdot}0$ s during damage evolution with initial damage of 0·1 in rock foundation elements

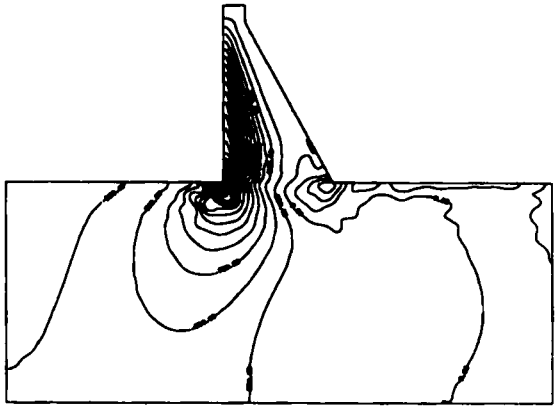

Figure 18(a). Major principal stress contour at time $t = 4{\cdot}46$ s without damage evolution and initial damage

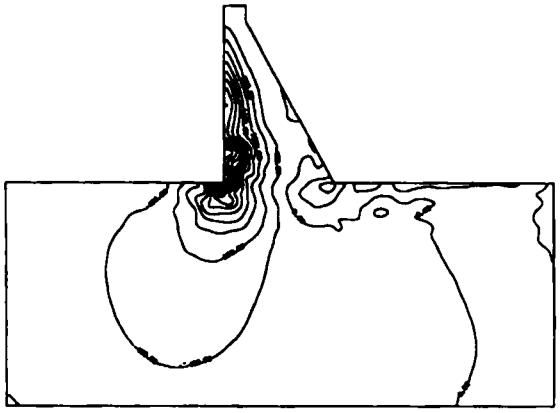

Figure 18(b). Net major principal stress contour during damage evolution without initial damage

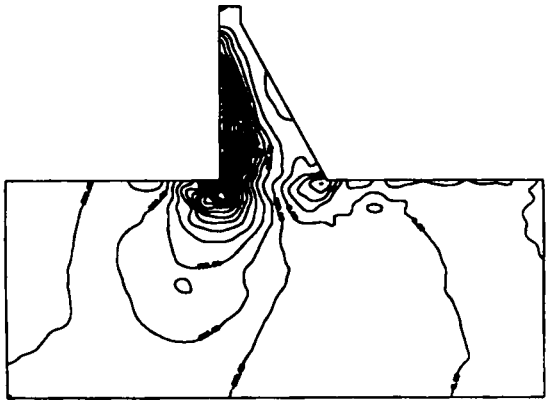

Figure 18(c). Net major principal stress contour at time $t = 4{\cdot}46$ s during damage evolution with initial damage in some areas according to Figure 9

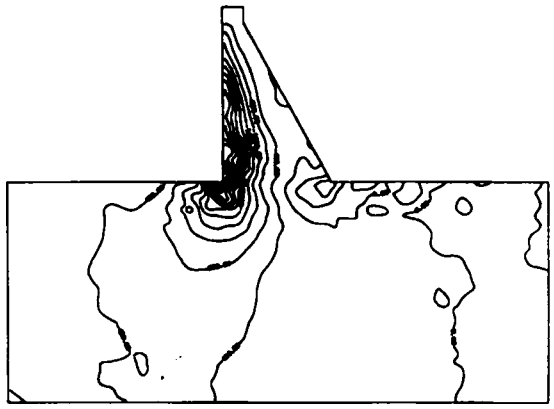

Figure 18(d). Net major principal stress contour at time $t = 4{\cdot}46$ s during damage evolution with initial damage of 0·1 in foundation rock elements

9. CONCLUSIONS

A computational method is presented for the dynamic response and damage analysis of concrete gravity dams with and without initial microcracks. A damage model for brittle materials exhibiting strain-rate-dependent fracture behaviour has been developed. Because concrete is an elastic-brittle material under seismic loading, the damage model developed here is appropriate. The model is capable of describing the rate-dependent non-linear behaviour of the brittle materials. Damage is defined as an internal state variable as well as a second-order tensor for anisotropic damage. Damage evolution based on power function of tensile principal stress is employed here to calculate the accumulated damage. Damage accumulation is reflected by the continuous degradation of material stiffness during the loading process.

Because of the statistical nature of the distribution of the microcracks, two-parameter Weibull distribution was assumed in the model to correct the experimentally measured material properties in order to account for sample size effects. Constants for the damage evolution law can be determined from laboratory data characterizing failure stress as a function of the strain rate.

The constitutive model together with damage evolution law have been implemented in the Lagrangian dynamic finite element program. The formulation has been applied to analyse a concrete gravity dam under seismic loading. The modelling of jointed rock mass using continuum damage mechanics is also presented together with the effect of soil–structure interaction. From the numerical examples, it can be observed that the seismic response of a damaged concrete dam could be significantly different from the undamaged dam. A damaged dam would have a higher amplitude and a higher level of stress. The results of the analysis indicate that the seismic waves travelling through a gravity dam would increase the magnitude of stresses in the damaged zones or in the local regions surrounding cracks and defects. In particular, the analysis shows that during a seismic event, the microstructure of a system can significantly change due to growth and propagation of microcracks.

REFERENCES

1. J. L. Hinks and E. M. Gosschalk, 'Dams and earthquakes – a review', *Dam Eng.* **IV(1)**, 9–26 (1993).
2. J. Zhou and G. Lin, 'Seismic fracture analysis and model testing of concrete gravity dams', *Dam Eng.* **III(1)**, 35–48 (1992).

3. J. F. Chappel and A. P. Ingraffea, 'A fracture mechanics investigation of the cracking of Fontana dam', *Department of Structural Engineering Report 81–87*, School of Civil and Environmental Engineering, Cornel University, Ithaca, New York, 1981.
4. P. Skrikerud, 'Discrete crack modelling for dynamically loaded, unreinforced concrete structures', *Earthquake eng. struct. dyn.*, **14**, 297–315 (1986).
5. R. H. Graves and K. N. Derucher, 'Interface smeared crack model analysis of concrete dams in earthquakes', *J. eng. mech. ASCE*, **113**, 1678–1693 (1987).
6. M. L. Ayari and V. E. Saouma, 'A fracture mechanics based seismic analysis of concrete gravity dams using discrete cracks', *Eng. Fracture Mech.*, **35**, 587–598 (1990).
7. E. P. Fahrenthold, 'Dynamic fracture of brittle anisotropic solids, in: J. W. Ju *et al.* (eds), *Damage Mechanics in Engineering Materials*, 1990, pp. 251–262.
8. S. Valliappan, 'Analysis of anisotropic damage mechanics problems', in: S. N. Atluri *et al.* (eds), *Proc. Int. Conf. on Computational Engineering Science*, Melbourne, Australia, 1991, pp. 1142–1147.
9. J. Lemaitre and J. L. Plumtree, 'Application of damage concepts to predict creep-fatigue failures', *J. Eng. Mater. Trans. ASME*, **101**, 284–292 (1979).
10. S. Valliappan, V. Murti and W. Zhang, 'Finite element analysis of anisotropic damage mechanics problems', *Eng. Fracture Mech.*, **35**, 1061–1071 (1990).
11. M. Yazdchi, S. Valliappan and W. Zhang, 'A continuum model for dynamic damage evolution of anisotropic brittle materials', *Int. J. numer. methods eng.*, **39**, 1555–1583 (1996).
12. L. M. Kachanov, 'Continuum model of medium with crack', *J. eng. mech. ASCE*, **106**, 1039–1051 (1982).
13. J. H. Yon, 'Dynamic fracture of concrete', *Ph.D. Thesis* University of Washington, U.S.A., 1990.
14. C. Georgiadis, 'Probability of failure models in finite element analysis of brittle materials', *Comput. Struct.*, **18**, 537–549 (1984).
15. W. Weibull, 'A statistical distribution function of wide applicability', *J. appl. mech. ASME*, **18**, 293–297 (1951).
16. B. Steverding, 'Dynamic weibull law', *Int. J. Fracture Mech.*, **5**, 243–244 (1969).
17. W. H. Dukes, *Handbook of Brittle Material Design Technology*, North Atlantic Treaty Organization, Advisory Group for Aerospace Research and Development AGARDograph, 1970.
18. K. F. Graff, *Wave Motion in Elastic Solids*, Oxford University Press, Oxford, 1975.
19. B. Haggblad and G. Nordgren, 'Modelling nonlinear soil–structure interaction using interface elements, elastic-plastic soil elements and absorbing infinte elements', *Comput. Struct*; **26**, 307–324 (1987).
20. P. Bettess, *Infinite Elements*, Penshaw Press, 1992.
21. W. White, S. Valliappan and I. K. Lee, I. K., 'Unified boundary for finite dynamic models', *J. eng. mech. ASME*, **103** (EM5), 949–964 (1977).
22. J. Lysmer and R. L. Kuhlemeyer, 'Finite dynamic model for infinite media', *J. eng. mech. ASCE.*, **95**, (EM4), 859–877 (1969).
23. S. Valliappan, W. White and I. K. Lee, 'Energy absorbing for anisotropic material', in: C. S. Desai, (ed.), *Proc. 2nd Int. Conf. on Numerical Methods in Geomechanics*, Blacksburg, 1976, pp. 1013–1024.
24. O. C. Zienkiewicz, *The Finite Element Method*, McGraw-Hill, London, 1977.
25. T. Kawamoto, Y. Ichikawa and T. Kyoya, 'Deformation and fracturing behavior of discontinuous rock mass and damage mechanics theory', *Int. J. numer. analyt. methods geomech.*, **12**, 1–30 (1988).
26. C. S. Desai, H. M. Galagoda and G. W. Wathugala, 'Hierarchical modelling for geologic materials and discontinuities-joints, interfaces', in: C. S. Desai *et al.* (eds), *Proc. 2nd Int. Conf. Constitutive Laws for Engineering Materials: Theory and Applications*, Arizona, U.S.A., 1987, pp. 81–94.
27. H. F. Schweiger, W. Haas and E. Handel, 'A thin-layer element for modelling joints and faults', in H. P. Rossmanith (ed.), *Proc. Int. Conf. on Mechanics of Jointed and Faulted Rock*, Vienna, Austria, 1990, pp. 559–564.
28. P. A. Cundall, 'A computer model for simulating progressive large scale movements in blocky rock systems', *Proc. Symp. of the Int. Society of Rock Mechanics*, Nancy, France, 1, Paper No. II-8, 1971.
29. D. Krajcinovic and M. Silva, 'Statistical aspects of the continuous damage theory', *Int. J. Solid Struct.* **18**, 551–562 (1982).